

The Radiation Response of Capacitors Fabricated on Bonded Silicon-On-Insulator Substrates¹

P. J. McMarr², B. J. Mrstik, R. K. Lawrence³, and G. G. Jernigan

Code 6816, Naval Research Laboratory, Washington, DC 20375

³ARACOR/SFA, Washington, DC 20375

Abstract

Silicon-on-insulator substrates were manufactured by bonding a thermal oxide of silicon to a silicon wafer. Metal-oxide-silicon capacitors were fabricated on these substrates. Capacitors were also fabricated on unbonded thermal oxides. Capacitance-voltage measurements were performed on the bonded and unbonded oxides, before and after 10 keV x-ray irradiation. The flatband shift for the irradiated bonded oxide was nearly double that of the irradiated unbonded oxide. The radiation-induced shifts of the capacitance-voltage curves are shown to be related to the density differences between the bonded and unbonded oxides.

I. INTRODUCTION

Metal-oxide-silicon (MOS) devices fabricated on silicon-on-insulator (SOI) substrates show enhanced resistance to single event upset compared to devices fabricated on bulk silicon [1]. Any radiation-induced charge trapped in the insulator may, however, result in shifts in the threshold voltages of the MOS devices [2]. In previous studies of SOI substrates formed using the SIMOX process, Mrstik et al. demonstrated that changes in the density of the insulator were related to changes in the radiation-induced charge trapped in the insulator [3,4].

In the present study this previous work is extended to include UNIBOND[®] SOI substrates formed using the SMART-CUT[®] process [5,6]. Spectroscopic ellipsometry measurements were performed on these substrates. These measurements were used to determine the density of the insulator. Metal-oxide-silicon capacitors were fabricated and capacitance-voltage (CV) measurements were performed before and after x-ray irradiation. The relationship between the flatband shifts measured from the CV curves and the density of the insulator for these substrates was established. The fabrication process parameters that result in changes in the density of the insulator were determined. Infrared transmission spectroscopy measurements were used to examine strain in the oxides used in the SMART-CUT process and in the UNIBOND buried oxide. The stoichiometry of the oxides was measured using x-ray photoelectron spectroscopy (XPS).

¹This work was supported by the Defense Special Weapons Agency.

²SFA, Inc., Landover, MD 20785.

⁴UNIBOND[®] and SMART-CUT[®] are registered trademarks of SOITEC SA.

II. EXPERIMENTAL DETAILS

A. Fabrication of Silicon-On-Insulator Substrates

In this study SOI substrates were formed using a process that relies on implantation and bonding, the SMART-CUT (SOITEC) process (Fig. 1) [5,6]. A thermal oxide of silicon is first grown on one wafer. Hydrogen ions are implanted through the oxide to a predetermined depth in the wafer (Wafer A in Fig. 1 (a)). The energy selected for implantation determines the depth in the silicon wafer at which the majority of the hydrogen is located. This leaves a relatively hydrogen free silicon region below the thermal oxide (in Fig. 1(a) this is labeled "TOP SILICON"), a heavily hydrogen implanted silicon region, and the silicon wafer. An additional silicon wafer ("Si WAFER B" in Fig. 1 (b)) is bonded to the thermal oxide of the implanted wafer.

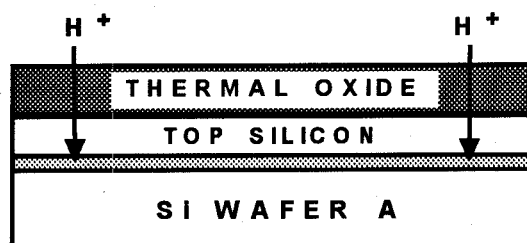


Figure 1 (a). Hydrogen ions are implanted through a thermal oxide of silicon into the silicon wafer.

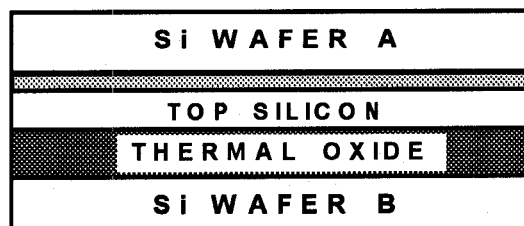


Figure 1 (b). The H⁺ implanted wafer is rotated 180° and the thermal oxide is hydrophilically bonded to an additional silicon wafer.

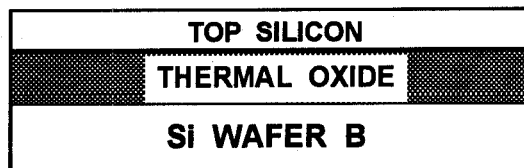


Figure 1 (c). Finished UNIBOND silicon-on-insulator substrate.

A two step thermal cycle is then applied. In the first thermal cycle the bonded wafers are annealed at $\sim 600^\circ\text{C}$. The bulk of the implanted wafer delaminates along the region defined by the hydrogen implantation profile. This results in a thin top silicon layer on top of a thermal oxide on a silicon substrate. In the second thermal cycle the SOI substrate is annealed at $\sim 1150^\circ\text{C}$ in an argon ambient. To remove any roughness from the thin top silicon layer, a final CMP process is used. The finished SOI substrate is referred to as UNIBOND (Fig.1 (c)).

The SMART-CUT process starts with a thermal oxide. SOITEC supplied the Naval Research Laboratory with their typical starting thermal oxides. In the text this is referred to as thermal oxide. SOITEC also supplied oxides that comprise all stages of the SMART-CUT process. The names used in the text to describe the other oxides are labelled with the processing steps to which they were subjected. The authors examined the thermal oxide, the H^+ implanted, bonded, and split thermal oxide (600°C anneal), and several UNIBOND oxides from different wafers (thermal oxide, H^+ implanted, bonded, split (600°C anneal), and then further annealed at 1150°C).

B. Spectroscopic Ellipsometry Measurements

Spectroscopic ellipsometry measures, as a function of wavelength (photon energy eV), the complex Fresnel reflectance ratio r given by the following equation

$$r = r_p/r_s = \tan\Psi \exp(i\Delta)$$

where r_p and r_s are the complex reflection coefficients for light polarized parallel and perpendicular to the plane of incidence. Ellipsometry data is usually given in terms of Δ and Ψ and in this work will be presented in that format [7].

Since the reflection phase difference (Δ) and amplitude ratio (Ψ) are both measured, it is generally possible to determine two material parameters of the system under study. These parameters could, for example, be the optical properties of an absorbing substrate (the real and imaginary parts of the complex dielectric function). As will be discussed further, the two material parameters that are determined in the present study are the thickness and the refractive indices of the oxides used in the SMART-CUT process [8]. A typical spectroscopic ellipsometry measurement on the buried oxide of a UNIBOND substrate is shown in Fig. 2.

C. Stylus Profilometry Measurements

The thickness of the UNIBOND buried oxide and the oxides used in the SMART-CUT process were also measured using stylus profilometry. The stylus profilometer used in these measurements was a TENCOR 250 with a submicron tip. The stylus pressure employed was less than 2 mg and the scan length selected was 400 mm. In order to perform the profilometry measurements, steps to the substrate silicon were fabricated on the oxides using conventional lithographic

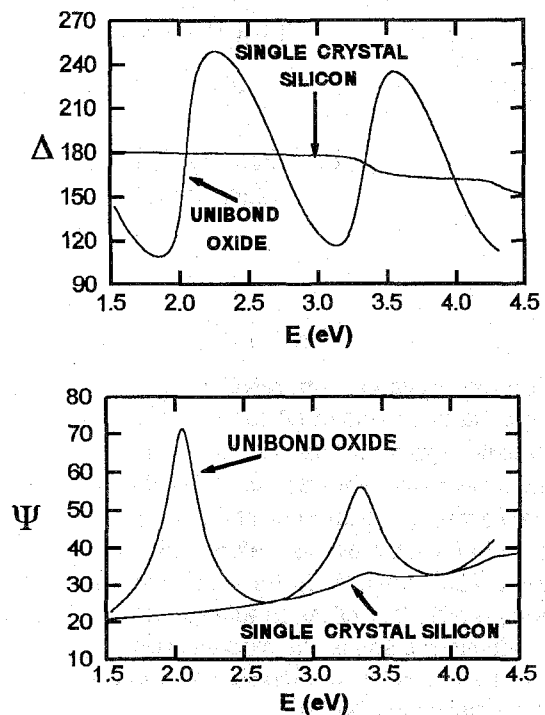


Figure 2. Δ (phase difference) and Ψ (amplitude ratio) from spectroscopic ellipsometry measurements performed at an angle of incidence of 61.42° .

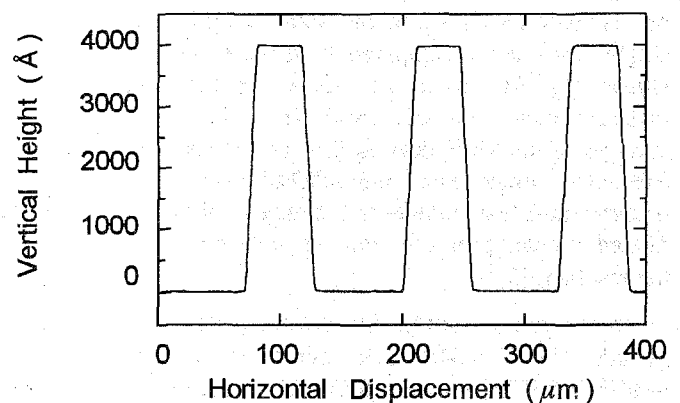


Figure 3. Typical stylus profilometry scan of an oxide used in the SMART-CUT process.

techniques. A profilometry scan of the oxide steps is shown in Fig. 3. The thickness of the oxide for this scan was determined from least squares fitting of the three steps shown in the figure.

The standard procedure was to perform twenty-five scans (each consisting of three steps) at approximately equally spaced intervals on a 1 cm^2 oxide sample. The results of this procedure are shown for two oxides in Fig. 4. The average of the profilometry measurements on these regions was then defined as the profilometry oxide thickness. The standard deviation of the thickness values of the oxides from these measurements was $\sim 10\text{ Å}$. This value was constant for all the oxides studied and probably results from roughness of the silicon substrate.

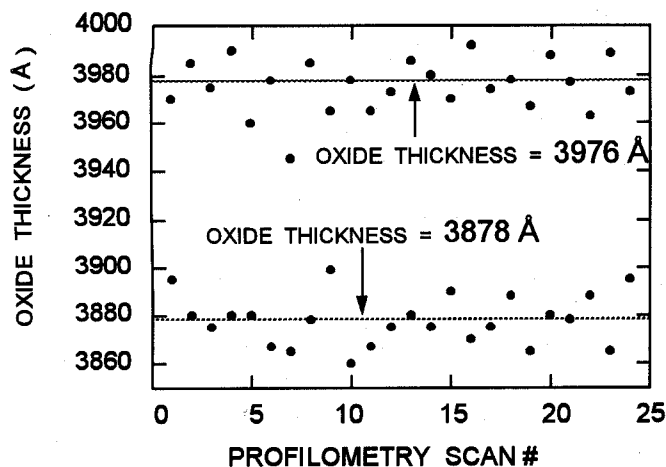


Figure 4. Thickness values of two oxides measured using stylus profilometry.

D. Infrared Transmission Measurements

Infrared transmission measurements were performed on the oxides using a Nicolet Model 750 FTIR Spectrometer. The resolution selected was 4 cm^{-1} . This value was selected as a compromise between intensity through the instrument and the resolution necessary to determine any differences in the spectra of the oxides. The background spectrum was that of the silicon substrate on which the oxides were grown. Fig. 5 is an example of the spectra measured on this instrument.

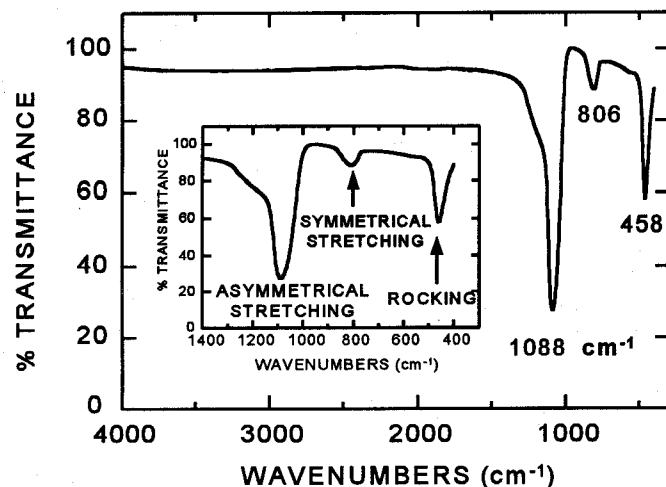


Figure 5. Infrared transmission measurements of the starting thermal oxide of the SMART-CUT process.

Included in the figure are assignments for each of the three major TO absorption bands which are characteristic of particular vibrational modes of the oxygen atoms with respect to the silicon atom pairs which they bridge. Rocking of the oxygen atoms about an axis through the two silicon atoms characterizes the vibrational behavior of the lowest frequency TO band (458 cm^{-1}). Symmetrical stretching of the oxygen atom along a line bisecting the axis formed by the two silicon atoms characterizes the band at 806 cm^{-1} , while the mode at 1088 cm^{-1} (and its high frequency shoulder) are due to an

asymmetrical stretch motion in which the oxygen atoms move back and forth along a line parallel to the axis through the two silicon atoms [9].

E. X-ray Photoelectron Spectroscopy Measurements

X-ray photoelectron spectroscopy was used to determine the stoichiometry of the oxides used in the SMART-CUT process and the buried oxide of the UNIBOND substrate. Spectra were acquired using a VG ESCALab Mark II. The system consists of a twin Al/Mg x-ray anode, a hemispherical electron energy analyzer, and a Leybold Heraeus sputter gun and scan unit. The Mg x-ray anode was operated at a 15 kV potential and a 20 mA emission current. Photoelectrons were accepted through a 3 mm slit in the analyzer which was operated with a 50 eV pass energy. Data was acquired of the Si 2p, O 1s, and C 1s regions in 0.1 eV steps. Spectra for the thermal oxide (the starting point of the SMART-CUT process) are shown in Fig. 6.

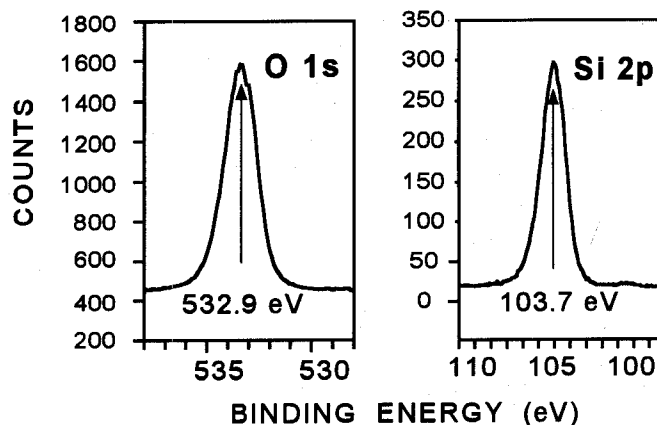


Figure 6. X-ray photoelectron spectroscopy spectra of the starting thermal oxide used in the SMART-CUT process.

F. Capacitance-Voltage Measurements and Radiation Testing

The UNIBOND substrates chosen for study were p-type ($14\text{--}22\ \Omega\text{cm}$). The top silicon layer was $\sim 2000\text{ Å}$ thick and the buried oxide was $\sim 4000\text{ Å}$. Aluminum was deposited on the top silicon in the form of circular pads with an area of 0.005 cm^2 . These samples were then placed in hydrazine, a highly specific silicon etch. This procedure produced silicon-insulator-silicon (SIS) devices. Metal-oxide-silicon capacitors were also fabricated (the top silicon was removed using hydrazine).

The SIS devices and MOS capacitors formed on these samples were irradiated using a 10 keV x-ray source ($1800\text{ rad (SiO}_2\text{)/sec}$) under a low field bias of $+5\text{ E } 4\text{ V/cm}$ [10] (with reference to the top silicon or oxide) to a total dose of 1 Mrad. One megahertz CV measurements were performed on the pre- and post-irradiated devices. Figure 7 (a,b) show these measurements for a UNIBOND MOS capacitor.

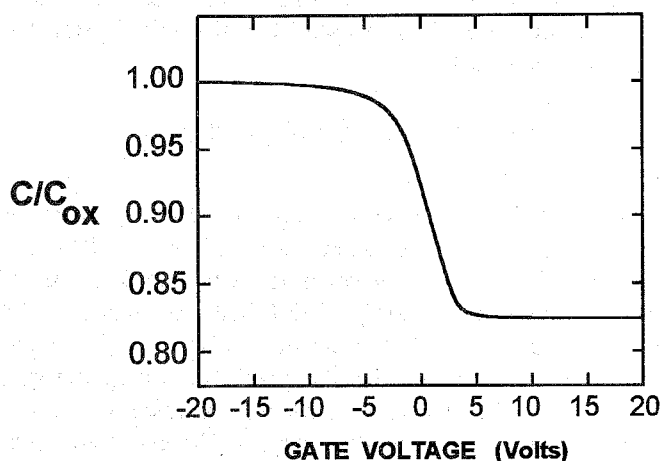


Figure 7 (a). Preirradiation 1 Mhz capacitance-voltage measurements on a UNIBOND oxide.

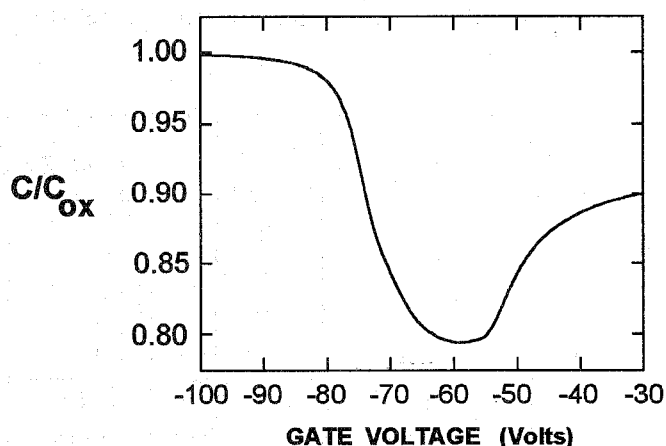


Figure 7(b). Postirradiation 1 Mhz capacitance-voltage measurements on UNIBOND oxide (dose = 1 Mrad, field = + 5 E 4 V/cm).

A. Radiation Response

Figure 7 (b) shows that net positive charge is present in the UNIBOND oxide following irradiation. As shown in Fig. 1, the UNIBOND oxide has been implanted with hydrogen, bonded, annealed at 600 °C, subjected to stresses during splitting, and further annealed to 1150 °C. Any of these processes may affect the radiation induced charge trapping properties of the oxide.

In order to understand which SMART-CUT processing parameter had the major effect on the charge trapping properties of the oxide, it was necessary to examine the radiation response of the oxide at each step in the process. As discussed previously, SOITEC supplied the Naval Research Laboratory with wafers from each step of the SMART-CUT process. The wafers of particular interest are: (1) the starting thermal oxide, (2) the H⁺ implanted thermal oxide, (3) the H⁺ implanted, bonded, and split wafer, and (4) several UNIBOND wafers

MOS capacitors (and SIS devices where possible) were fabricated on these particular samples. Capacitance-voltage

measurements were performed. The CV curves for the thermal oxide, and (see Fig. 7 (a)) the UNIBOND oxide were acceptable, with minimum hysteresis. However, the CV curve for the H⁺ implanted thermal oxide showed no depletion or inversion, probably as a result of implantation damage at the SiO₂/Si interface.

The CV curve for the H⁺ implanted, bonded, and split oxide showed massive hysteresis that was dependent upon the sign and magnitude of the final value of the gate voltage. This behavior is possibly caused by residual H⁺ trapped in the oxide that is moving in response to the field and is currently under study [11].

Therefore, of all the wafers available, only the thermal oxide and UNIBOND oxide were acceptable for radiation testing. These were insufficient to determine which SMART-CUT processing steps influence the radiation sensitivity of the UNIBOND oxide. To circumvent this limitation annealing studies were conducted on the thermal oxide, the H⁺ implanted thermal oxide, and the H⁺ implanted, bonded, and split oxide. This last sample was annealed with and without the top silicon in place (hydrazine was used to remove the top silicon).

These samples were annealed at temperatures from 700 °C to 1150 °C in fused quartz and polysilicon furnaces using MOS grade argon. They were ramped up to the annealing temperature in 100 °C increments in 30 minutes, held at the annealing temperature for 60 minutes, and then cooled in 100 °C increments to room temperature in 30 minutes. Metal-oxide-silicon capacitors were fabricated and CV measurements were performed.

Capacitance-voltage curves could not be obtained on the H⁺ implanted, annealed thermal oxide. Current-voltage measurements showed that a conductive path existed from the aluminum metal to the substrate silicon. Nomarski microscopy and stylus profilometry measurements revealed that large regions of the oxide were missing. Apparently, when no bonded wafer is present, the expanding implanted hydrogen exerts sufficient force on the oxide to cause delamination of the oxide from the silicon wafer.

The samples available for radiation testing were: (1) the unannealed and annealed thermal oxides, (2) the annealed H⁺ implanted, bonded, and split oxides, and (3) the UNIBOND oxide. Twenty MOS capacitors (or SIS) devices were irradiated on each oxide. Stretchout was not a problem with any of the postirradiation CV curves (Fig. 7(b)), and the flatband voltage was selected as a reference for comparing the radiation response of the various samples. The standard deviation of the flatband voltage shifts was ~ 5 volts. The average flatband shifts for these samples are shown in Figs. 8 and 9.

Figure 8 shows the flatband shift for the 700 °C annealed H⁺ implanted, bonded, and split oxide. As discussed previously, the CV curve for the H⁺ implanted, bonded, and split (600 °C anneal) oxide exhibited unacceptably large

hysteresis. A 60 minute argon anneal at 700 °C reduced the hysteresis to less than 5 volts. This is still too large for real device fabrication but acceptable for radiation testing. The flatband shift for the 700 °C sample shown in Fig. 8 was measured on samples which were annealed with the top silicon in place. The results were identical for samples with the top silicon removed prior to annealing.

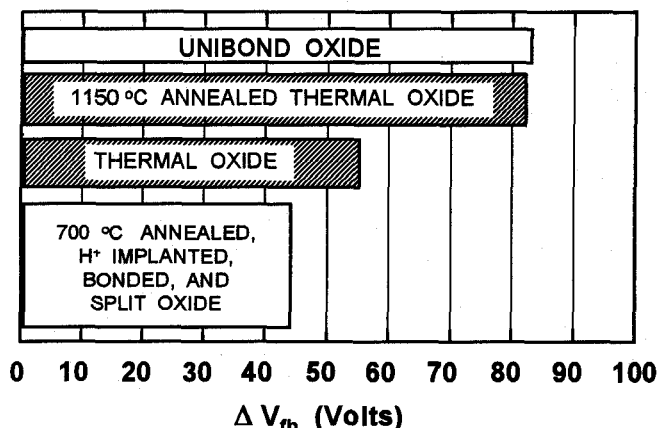


Figure 8. Flatband shifts for the oxides used in the SMART-CUT process (dose = 1 Mrad, field = + 5 E 4 V/cm).

The flatband shift for the starting thermal oxide is 54 volts. An additional thermal oxide from the same wafer was annealed in argon to 1150 °C and had a flatband shift of 82 volts. As shown in Fig. 8, the flatband shift for the annealed thermal oxide and the UNIBOND oxide (1150 °C bond anneal) are nearly identical.

On the basis of these results further radiation testing was performed on the H⁺ implanted, bonded, and split oxides annealed at temperatures from 700 °C to 1150 °C. The results of the CV measurements on these samples are shown in Fig. 9. As the anneal temperature increases from 700 °C to 800 °C there is an increase in the flatband voltage shift of ~ 10 volts. Further increases in the anneal temperature result in incremental changes in the flatband voltages of ~ 5 volts.

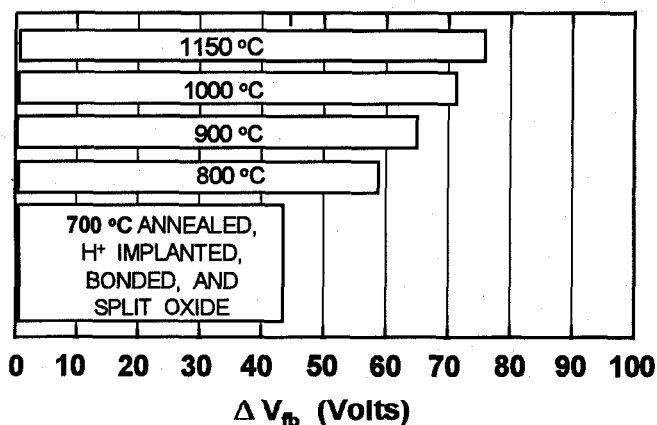


Figure 9. Flatband shifts for the H⁺ implanted, bonded, and split oxides which were further annealed from 700 °C to 1150 °C.

The results in Figs. 8 and 9 suggest that that the main SMART-CUT processing parameter responsible for the radiation response of the UNIBOND oxide is the high temperature anneal (1150 °C) that is used by SOITEC to form this SOI substrate. This statement is based on the observation that the flatband shift for the 1150 °C annealed starting thermal oxide and the flatband shift for the UNIBOND oxide are statistically the same under the field (+5 E 4 V/cm), dose (1 Mrad), and dose rate (1800 rad (SiO₂)/sec) used in these experiments.

Capacitance-voltage measurements performed on the H⁺ implanted, bonded, and split oxides annealed at 800 °C (and higher temperatures) showed little or no hysteresis before and after irradiation. In terms of minimal radiation response with good CV characteristics, the H⁺ implanted, bonded, and split oxide annealed at 800 °C is an adequate SOI substrate with a flatband shift ~ 20 volts less than the UNIBOND oxide (Fig. 9). The flatband shifts for the oxides annealed at temperatures less than 1150 °C are substantially different from that of the starting thermal oxide. The radiation sensitivity of these oxides was obviously influenced by the H⁺ implantation, bonding, and splitting. However, an 1150 °C anneal eliminates the effect the processing parameters have on the radiation sensitivity of these oxides.

B. Spectroscopic Ellipsometry Results

In previous studies Mrstik et al. established a relationship between the flatband shift of MOS capacitors fabricated on SIMOX buried oxides (irradiated using the same conditions as the SMART-CUT oxides) and the density of the buried oxides [3,4]. The density values for the SIMOX oxides were determined from analysis of spectroscopic ellipsometry measurements. To determine if a similar relationship holds for the SMART-CUT oxides, spectroscopic ellipsometry measurements were performed on the same samples as those used in the capacitance-voltage measurements.

The refractive indices for the oxides, determined from an analysis of the spectroscopic ellipsometry measurements, are shown in Fig. 10. The refractive indices for the 1150 °C annealed thermal oxide and the UNIBOND oxide are the same. The refractive indices of the 1150 °C annealed starting thermal oxide are lower than the starting thermal oxide. The refractive indices for the UNIBOND oxide are lower than those of the H⁺ implanted, bonded, and split oxide. These results are significant since (1) they demonstrate that a relaxation process occurs when the starting thermal oxide is subsequently annealed at 1150 °C [12] and (2) they show that the UNIBOND oxide does not undergo any thermally induced degradation from the 1150 °C anneal (which would increase the refractive indices as compared to the starting thermal oxide). In addition, the fact that the refractive indices for the UNIBOND oxides are the same as those for the 1150 °C annealed starting thermal oxide suggests that the only processing step responsible for the refractive indices of the

UNIBOND oxide is the 1150 °C anneal used to form the UNIBOND oxide.

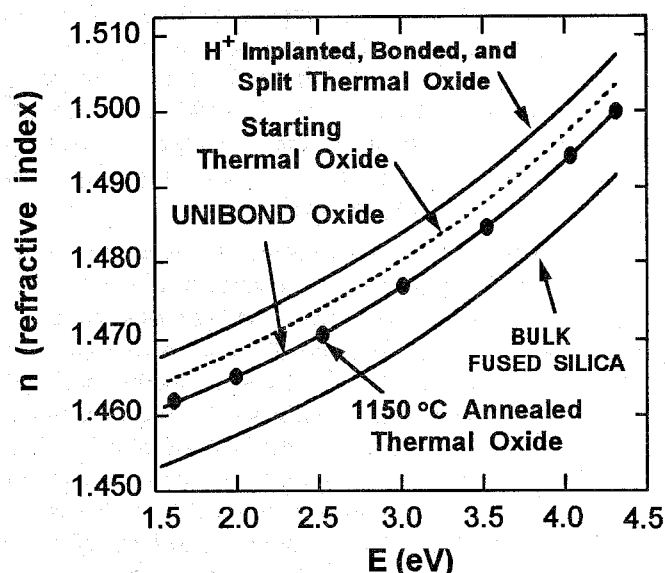


Figure 10. Refractive indices (n) for the H^+ implanted, bonded, and split oxide (top curve), starting thermal oxide (dashed line), UNIBOND oxide (middle curve), 1150 °C annealed starting thermal oxide (solid circles), and bulk fused silica (bottom curve).

The refractive indices of silicon oxides are a measure of the relative polarizabilities of the oxides. The polarizability of the oxides results from the local atomic configuration and the network structure of the oxides. The network is composed of tetrahedra linked together in ring structures. If the refractive indices decrease following postoxidation processing, then tetrahedra linked in smaller rings relink to form larger rings and the net polarizability of the oxide (or the refractive indices) decrease. The density of the oxide decreases. To interpret the spectroscopic ellipsometry measurements using this model, the authors use the Bruggeman effective medium model [13]. The density values for the SMART-CUT and UNIBOND oxides using this model are shown in Fig. 11.

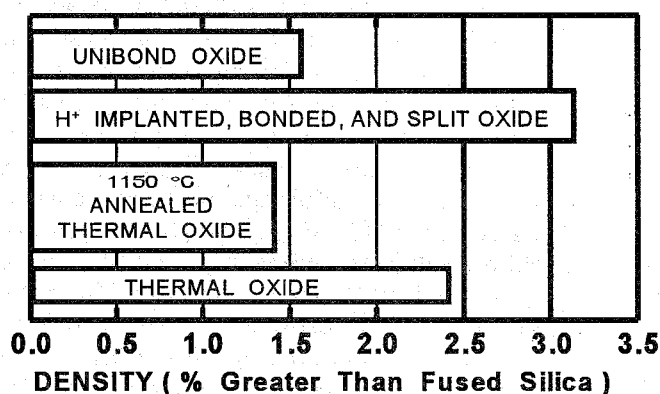


Figure 11. Density values (percent greater than fused silica) for the oxides used in the SMART-CUT process.

In Fig. 11 the values of the density for the samples are shown with reference to those of fused silica. The Bruggeman model requires reference dielectric function data for one of the end members. The density values are then referenced to the density of this end member. Fused silica was chosen, since (from Fig. 10) it has the lowest refractive indices of all the samples and the optical and dielectric constants are remarkably constant regardless of manufacturer. The density of this material is well known and the density values in Fig. 11 could be absolutely referenced. However, it is common practice in the use of effective medium models to present the values in the form shown in the figure.

The density values for the 1150 °C annealed thermal oxide and the UNIBOND oxide are nearly identical, at ~ 1.5% greater than fused silica. The H^+ implanted, bonded, and split oxide has the largest value at ~ 3% greater than fused silica. These results are based on a model which could be incorrect. If this model is applicable to the SMART-CUT oxides, and the refractive indices of these oxides decrease following a postoxidation anneal, then the oxide thicknesses must increase.

C. Stylus Profilometry, Infrared Spectroscopy, and XPS Results

To determine the validity of the authors interpretation of the spectroscopic ellipsometry measurements, two facts must be established: (1) if the refractive indices for a given sample decrease following postoxidation anneal, then the thickness of the oxide must increase, and (2) the oxides must be stoichiometric. The best sample of the SMART-CUT oxides to use for this test is the sample with the largest density. From Fig. 11 this is the H^+ implanted, bonded, and split oxide.

The top silicon was removed from this sample using hydrazine. Steps were etched to the substrate silicon and stylus profilometry measurements (as described in the *Stylus Profilometry Measurements* section) were used to determine the thickness of the oxide. An additional sample from the same wafer was then annealed at 800 °C for 60 minutes in argon (see the *Radiation Response* section for additional details on the annealing conditions) and steps were then fabricated on this oxide. Spectroscopic ellipsometry measurements were also performed on these identical samples necessarily before the steps were cut into the oxides. The results of the profilometry measurements are shown in Fig. 12.

The average profilometry thickness value of the pre-anneal oxide is 3878 Å, while that determined from spectroscopic ellipsometry measurements was 3886 Å. The profilometry value following the 800 °C anneal was 3940 Å, and the spectroscopic ellipsometry value was 3945 Å. Similar comparisons were made on the other oxides used in the SMART-CUT process. Since stylus profilometry is a direct (but necessarily destructive) measurement technique, the expansion of this and other samples following postoxidation

anneal is irrefutable. This is an unambiguous demonstration that a postoxidation anneal can result in an expansion of the oxide and has implications for any postoxidation annealing of silicon oxides used in semiconductor fabrication.

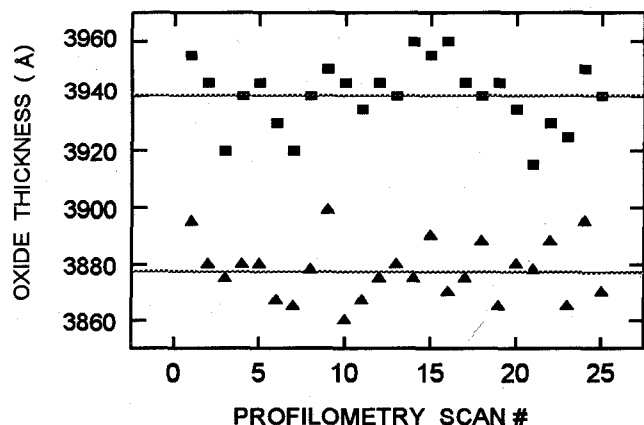


Figure 12. Thickness values of the H^+ implanted, bonded, and split oxide before the 800 °C anneal (triangles) and after the 800 °C anneal (squares).

Although not shown, the refractive indices for the 800 °C annealed, H^+ implanted, bonded, and split oxide decrease to values slightly lower than that of the starting thermal oxide (Fig. 10). These refractive index values are significantly lower than those of the unannealed, H^+ implanted, bonded, and split oxide. The authors interpret the decrease in the refractive indices following postoxidation anneal as a decrease in the polarizability of the oxide as smaller rings link to form larger ring structures with the consequent expansion of the oxide. The profilometry measurements demonstrate that a postoxidation anneal results in an expansion of the oxide and the very good agreement between the profilometry and spectroscopic ellipsometry measurements further establishes this fact.

The second point that must be demonstrated is that all the oxides used in the SMART-CUT process and the UNIBOND oxide are stoichiometric. Infrared spectroscopy [9] and x-ray photoelectron spectroscopy [14] are accepted techniques for determining the stoichiometry of silicon oxides. Using the instrument described previously (EXPERIMENTAL DETAILS, *Infrared Transmission Measurements*) infrared measurements were performed on all the oxides. Figure 13 shows the spectra for the H^+ implanted, bonded, and split oxide and the starting thermal oxide.

The asymmetrical stretching mode for the H^+ implanted, bonded, and split oxide is at 1061 cm^{-1} , while the starting thermal oxide is at 1088 cm^{-1} . The symmetrical stretching mode is displaced to 815 cm^{-1} compared to the thermal oxide at 806 cm^{-1} , while the rocking mode is shifted to 449 cm^{-1} from 458 cm^{-1} .

There are two possible interpretations of the infrared shifts for the H^+ implanted, bonded, and split oxide [9]. The first is that the implanted oxide is strained. The H^+ implantation has "pushed" the structure into a highly

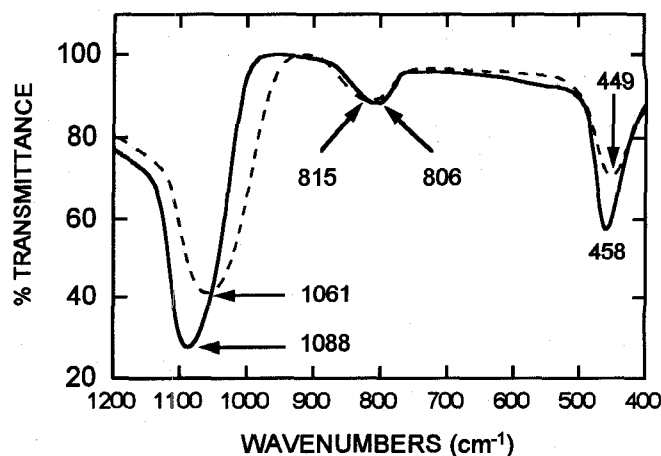


Figure 13. Infrared transmission spectra for the H^+ implanted, bonded, and split oxide (dashed), and the starting thermal oxide (solid).

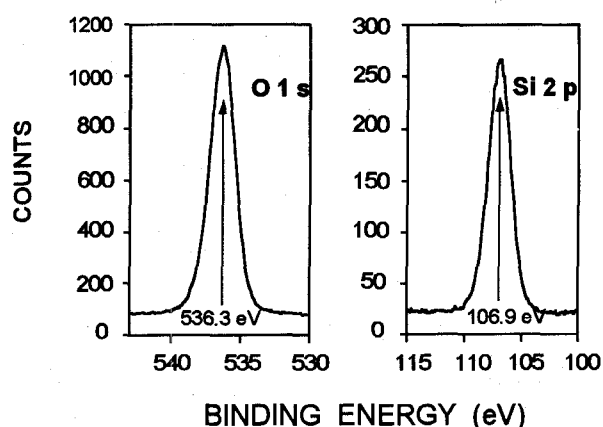


Figure 14. X-ray photoelectron spectroscopy spectra for the H^+ implanted, bonded, and split oxide.

compacted state, with the consequence displacement of the oxygen atoms from their preimplantation position. The second interpretation is that oxide is nonstoichiometric, with massive disruption of the SiO_2 network following implantation. To address this possibly XPS measurements were performed. The O 1s and Si 2p peaks are shown in Fig. 14.

The O 1s peak position is at 536.3 eV, while the Si 2p peak is at 106.9. This figure should be compared to the XPS spectra shown in Fig. 6 for the starting thermal oxide, where the O 1s peak is at 532.9 eV and Si 2p peak is at 103.7 eV. The peak positions for the H^+ implanted sample are shifted to higher binding energy values. Nonstoichiometry shifts the peak positions to lower binding energies [14]. The shift of the peak positions to higher energies as compared to the thermal oxide is possibly due to strain in the oxide or charging effects. Since the spectra for the thermal oxide are representative of spectra found in the literature for thermal oxides [14], the probable reason for the peak position shifts to higher energies is the presence of strain in the H^+ implanted, bonded, and split oxide, in exact agreement with the infrared transmission measurements.

The H^+ implanted, bonded, and split oxide is stoichiometric and highly compacted. This compaction increases the polarizability of the oxide and thus the refractive indices of the sample (Fig. 10). When this oxide is annealed to 1150 °C (i.e. annealed into a UNIBOND oxide) the XPS spectra is virtually identical to that of the starting thermal oxide.

IV. DISCUSSION

Mrstik et al. previously demonstrated that variations in the refractive indices for SIMOX oxides (and thermal oxides) result from density variations between the oxides. The density values of the oxides in these previous studies were determined from effective medium modeling of the spectroscopic ellipsometry measurements [3,4,8]. In the present work this procedure has been even more firmly established. The link between the density values determined from spectroscopic ellipsometry measurements of all the SMART-CUT oxides and the results from the CV measurements on these irradiated oxides is shown in Fig. 15.

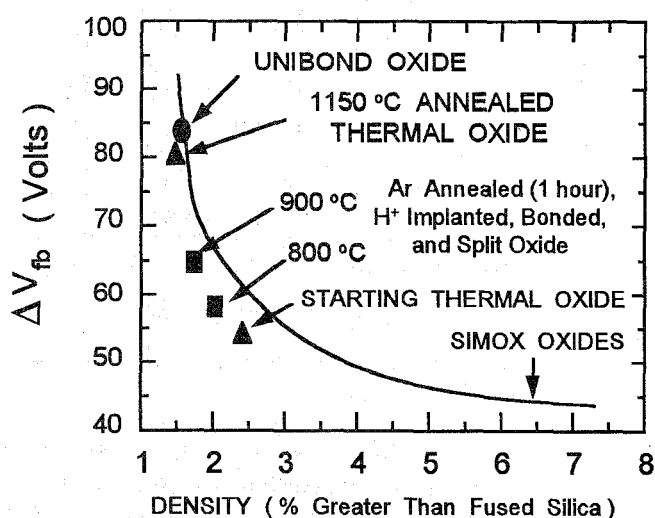


Figure 15. Average flatband shift vs. density for the H^+ implanted, bonded, and split oxides annealed at different temperatures, the starting thermal oxide, and SIMOX oxides (solid curve) [3,4]. (10 keV x-ray irradiation (1800 rad (SiO_2)/sec), dose= 1 Mrad, field = + 5 E 4 V/cm).

As the density of the oxides decreases, the radiation induced flatband shifts for the oxides increase. The density decrease for the annealed starting thermal oxide must result from an expansion of the oxide network. Smaller rings that make up the structure of the oxide link to form larger rings and the net polarizability of the oxide decreases. The increased radiation sensitivity of the annealed starting thermal oxide may result from broken Si-O bonds as the smaller rings link to form larger structures, or the larger rings may simply be more sensitive to radiation. The annealed starting oxide and the UNIBOND oxide are both stoichiometric but may contain unsatisfied Si bonds which can act as hole traps and the net positive trapped charge in

these oxides following irradiation is therefore larger as compared to that trapped in the starting thermal oxide. Additional experiments are in progress to determine the mechanisms responsible for the radiation sensitivity of the SMART-CUT substrates and postoxidation anneal sequences in general.

V. SUMMARY

In this study the authors have measured the radiation response of oxides used in the SMART-CUT process. The increased radiation sensitivity of oxides following a post-oxidation anneal has been correlated to an expansion of the oxides with consequent change in the densities of the oxides. These density differences are detectable using spectroscopic ellipsometry. Because of its sensitivity to the oxide density, spectroscopic ellipsometry should be useful in optimizing processing parameters to obtain the desired radiation response.

ACKNOWLEDGMENTS

The support of the Defense Special Weapons Agency is gratefully acknowledged. The authors also thank the members of SOITEC SA who supplied the wafers used in this study. In particular, the authors express their gratitude to A. Wittkower of SOITEC USA (Peabody, MA).

REFERENCES

- [1] A. J. Auberton-Herve, "SIMOX-SOI Technologies For High Speed and Radiation Hard Technologies: Status and Trends in VLSI and ULSI Applications," *Proc. 4th International Symposium on SOI Technology and Devices*, Electrochem. Soc. Vol. 90, No. 6, pp. 455-478, May 1990.
- [2] W. C. Jenkins and S. T. Liu, "Radiation Response of Fully-Depleted MOS Transistors Fabricated in SIMOX," *IEEE Trans. Nucl. Sci.*, Vol. 41, No. 6, pp. 2317-2321, December 1994.
- [3] B. J. Mrstik, P. J. McMarr, and R. K. Lawrence, "Relationship Between Radiation Response and Density of Buried Oxide in Separation-By-Implantation-Of-Oxygen Material," *Appl. Phys. Lett.*, Vol. 65, No. 5, pp. 2993-2995, December 1994.
- [4] B. J. Mrstik, P. J. McMarr, R. K. Lawrence, and H. L. Hughes, "The Use of Spectroscopic Ellipsometry to Predict the Radiation Response of SIMOX," *IEEE Trans. Nucl. Sci.*, Vol. 41, No. 6, pp. 2277-2283, December 1994.
- [5] M. Bruel, "Silicon-On-Insulator Material Technology," *Electronic Letters*, Vol. 31, No. 14, pp. 1201-1202, July 1995.

- [6] A. J. Auberton-Herve, J. M. Lamure, T. Barge, M. Bruel, B. Aspar, and J. L. Pelloie, "SOI Materials for ULSI Applications," *Semicond. Inter.*, Vol. 18, No. 11, pp. 97-104, October 1995.
- [7] R. M. A. Azzam and N. M. Bashara, Ellipsometry and Polarized Light, Amsterdam-New York-Oxford: North Holland Publishing Company, 1977.
- [8] B. J. Mrstik, P. J. McMarr, J. R. Blanco, and J. M. Bennett, "Measurement of the Thickness and Optical Properties of Thermal Oxides of Si Using Spectroscopic Ellipsometry and Stylus Profilometry," *J. Electrochem. Soc.* Vol. 138, No. 6, pp. 1770-1778, June 1991.
- [9] W. A. Pliskin and H. S. Lehman, "Structural Evaluation of Silicon Oxide Films," *J. Electrochem. Soc.* Vol. 112, No. 10, pp. 1013-1019, October 1965.
- [10] The theory for the selection of this field ($+ 5 \times 10^4$ V/cm) can be found in: J. H. Smith, R. Lawrence, and G. J. Campisi, "Numerical Analysis of Silicon-On-Insulator Short Channel Effects in a Radiation Environment," *J. Electron. Mat.* Vol. 21, No. 7, pp. 683-687, 1992.
- [11] This phenomena may be related to that described by: K. Vanheusden, W. L. Warren, R. A. B. Devine, D. M. Fleetwood, J. R. Schwank, M. R. Shaneyfelt, P. S. Winokur, and Z. J. Lemnios, "Non-volatile Memory Device Based on Mobile Protons in SiO_2 Thin Films," *Nature*, Vol. 386, pp. 587-589, April 1997.
- [12] C. S. Rafferty, L. M. Landsberger, R. W. Dutton, and W. A. Tiller, "Nonlinear Viscoelastic Dilation of SiO_2 Films," *Appl. Phys. Lett.*, Vol. 54, No. 2, pp. 151-152, January 1989.
- [13] D.A.G. Bruggeman, "Berechnung Verschiedener Physikalischer Konstanten von Heterogenen Substanzen," *Ann. Phys. (Leipzig)*, Vol. 24, pp. 636 - 640, December 1935.
- [14] F. J. Grunthaner and P. J. Grunthaner, "Chemical and Electronic Structure of the SiO_2/Si Interface," in *Material Science Reports*, Vol. 2-3, pp. 65-160, December 1986.